

Isolated Rotor in Vortex Ring State Aerodynamics Using CFD :

An investigation of the wind tunnel effect on vortex ring state aerodynamics

C. Castellin
Eurocopter S.a.S, Marignane, France

Abstract

The paper deals with the vortex ring state phenomenon occurring in the helicopter flight area corresponding to high rates of descent in vertical flight. It presents the CFD calculations performed to analyse the feasibility of wind tunnel tests to investigate this feature for an isolated rotor in vertical flight. A shape effect is done using a helicopter rotor type and a tilt rotor type. An investigation on the wind tunnel influence on this phenomenon is also presented for the helicopter rotor.

Nomenclature

C_T/σ : rotor thrust coefficient
 $Z_b = 200 C_T/\sigma$: non dimensioned thrust
 V_z : rate of climb/rate of descent
 V_{i0} : induced velocity of Froude

Introduction

The helicopter flight with high descending slopes is at the centre of many investigations. There is a huge interest to investigate this part of the flight envelope for both civil and military helicopters. Civil users look for potential reduction of the acoustic environmental impact around heliports, whereas military users can take benefit of manoeuvres with high descending slopes. In fact, this area of the flight envelope is not well known and therefore rarely used. The reason is the presence of the vortex ring state phenomenon which leads to dangerous flight conditions and then makes the flight tests difficult to be performed. Moreover, this complex aerodynamics phenomenon is often poorly modelled by the classical flight mechanical tools. The CFD tools developed by the French and German research centres (ONERA and DLR) and introduced in the industrial environment in the framework of the CHANCE program have been used to simulate the vortex ring state phenomenon for the descent in vertical flight. A first objective was to evaluate the capability of the elsA CFD code to predict the vortex ring state phenomenon. The second goal was to evaluate how the vortex ring state was affected

by the wind tunnel environment, and conclude on the feasibility of VRS tests in the Eurocopter Marignane wind tunnel.

The multiblock structured code elsA

The elsA solver is a multi-application object oriented aerodynamic code, which development started at ONERA in 1997. It is based on a cell-centred finite volume technique for structured multi-blocks meshes and includes a wide range of numerical techniques as well as physical models in order to simulate the flow-field around realistic aerospace configurations from the low subsonic to the hypersonic regime. The domain of application includes fixed wing, rotary wing, turbo-machinery, space launcher and missile configurations. In the present activity, the spatial discretisation used is the standard Jameson's second-order centred scheme with explicit artificial viscosity terms using second and fourth differences. A backward Euler explicit time integration technique is applied with a 4-stage Runge-Kutta algorithm, together with implicit residual smoothing. The implicit system is solved using LU decomposition.

Description of the hypothesis for the simulated configurations

The elsA code is used for the CFD simulation. In order to limit the CPU time consumption, only pure vertical flight was considered, where periodicity can be used as in the classical method for rotor performance computation in hover (Ref 1). So, one blade and the corresponding cylindrical area are modelled for the rotor. The calculations use the steady algorithm of elsA to simulate a steady configuration in the rotating frame. This assumption is also justified by the fact that no local flow separation is expected (limited rotor thrust), and that the high decrease of the thrust in the vortex ring state phenomenon is not linked to stall but to a recirculation phenomenon. The convergence of these steady calculations will confirm that the unsteadiness of the configuration is weak compared with the performance (thrust and

power) evolution through the vortex ring state phenomenon. The algebraic Michel turbulent model is used, which is sufficient for these configurations with an average thrust level ($C_T/\sigma=0.07$).

The blade is assumed to be rigid, to have no harmonic movements (pitch, flap and lag angles). The flap and the lag angles are also taken constant for all the collective pitch. Indeed the main interest is to investigate in the end the flight equilibrium for a constant helicopter mass versus the vertical velocity.

Description of the geometries for the simulated configurations

2 rotors have been considered. The first is the rotor of the powered model of the Dauphin AS365 helicopter and the second incorporates a tilt rotor blade with high twist (Fig 1). The blade sleeve has been considered for both rotors.

The wind tunnel considered in this analysis is the Eurocopter Marignane wind tunnel. The model is located inside an open jet test section as represented on figure 2.

For the free stream configuration the calculated area is a cylinder which diameter is equal to 12 times the blade span length and



Figure 1: Blade shapes

the height is equal to 15 times the blade span length.

In order to limit the number of grids and make easier the grid generation, the chimera technique has been used (Ref 2). One child grid for each blade and one background grid for each environment (free stream and wind tunnel) were thus necessary. An additional grid for the rotor disk area was derived from the free stream background grid and used with the wind tunnel configuration in order to have the same grid near the rotor disk as for free stream environment. Only five grids are then required to simulate all the configurations for the blade shape effect, the rotor polar versus collective pitch and the environment influence studies (Fig 3).

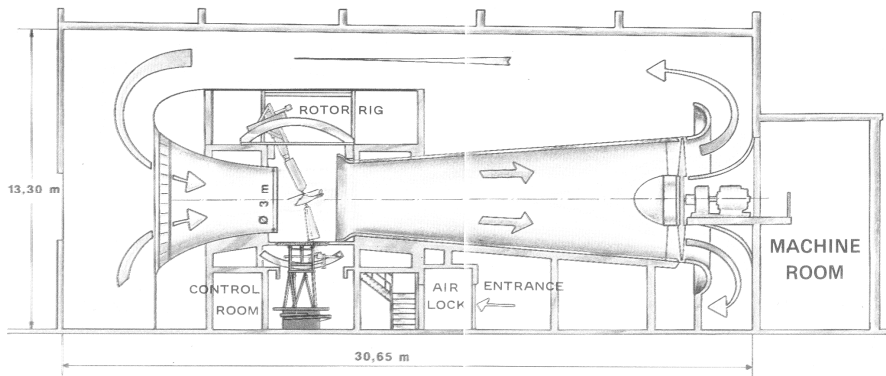


Figure 2 : Eurocopter Marignane Wind Tunnel

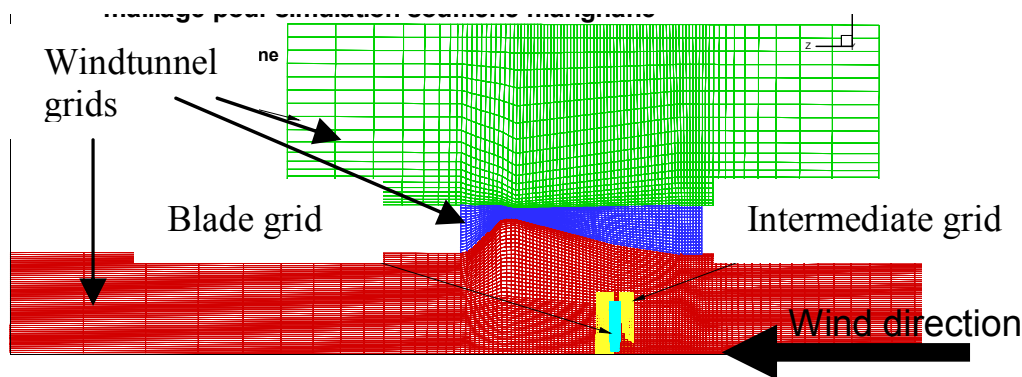


Figure 3 : Chimera construction for the wind tunnel configuration

Isolated rotors in free stream environment

For the AS365 rotor, some flight tests are available. The PhD thesis of J. JIMENEZ (Ref.3) is used for a qualitative validation of the first calculations on this rotor.

The extension of the fluid area represented by the grid for the free stream configuration is sufficient to use the classical 'far field' conditions instead of the 'Froude' conditions usually considered for the performance prediction of an isolated rotor in hover (Ref.4) in order to avoid recirculation due to the close grid boundaries. This allows having a good performance prediction in hover and for low rates of descent configurations, as well as using a unique set of boundary conditions for any rate of descent.

Around 4000 iterations are required to converge correctly for performance purpose outside the vortex ring state envelope whereas around 8000 iterations are required when this phenomenon occurs. This is due to the

recirculation which requires more time to converge. 8000 iterations have thus been finally performed for each calculation.

The rate of descent and the collective pitch were imposed and the result of the computation was the rotor thrust and the rotor power. The rate of descent was varied between 0 and 40 m/s in order to achieve a vertical velocity of around 2 times the mean Froude induced velocity. The pitch angles were taken between 8 and 14 degrees. The blade tip is the same for both rotors

The thrust calculated for each configuration is represented by contour levels on Figure 4, describing the computation range (rate of descent versus collective pitch). The nodes of the mesh give the calculation points. The vertical velocity is normalised by the Froude velocity in the hover reference thrust condition ($Z_b=15$).

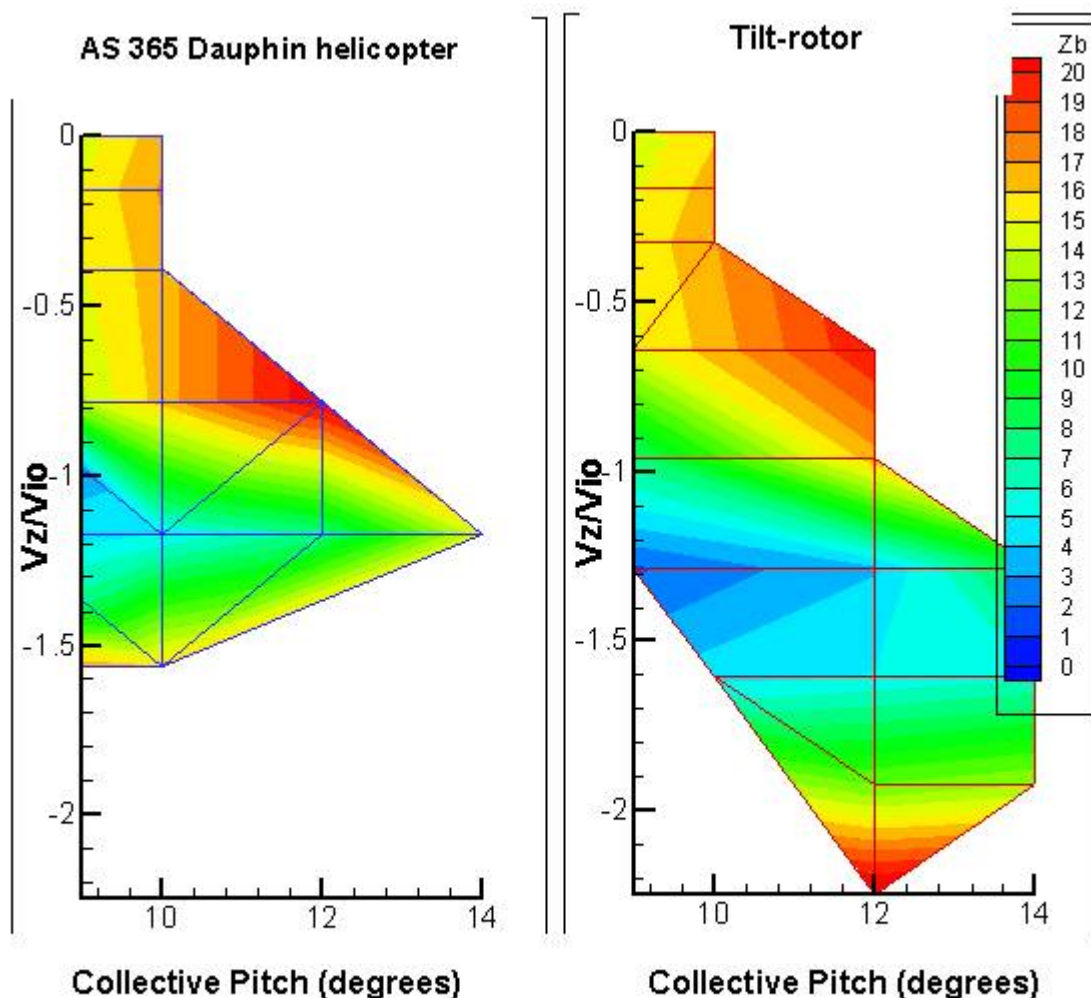


Figure 4 : Thrust (Z_b) calculated by CFD in free stream conditions - comparison of AS365 helicopter and tilt rotor

The curve for a given thrust value ($Z_b=15$ for example) provides the collective pitch evolution required as a function of the rate of descent in trim conditions :

1. In the very low rate of descent area starting from hover conditions, the "usual" trend can be seen: the collective pitch has to decrease to keep a constant thrust when the rate of descent increases. This is a stable phase: if the rate of descent increases with a fixed collective pitch, the thrust equally builds up, which leads to a reduction of the rate of descent.
2. When the vertical velocity is equal to around $-0.7 \cdot V_{i0}$ the collective pitch now needs to be increased to keep a constant thrust when increasing the rate of descent. The helicopter enters in an unstable range: increasing the rate of descent at a fixed collective pitch reduces the thrust and thus makes the rate of descent grow. This is the entrance in the vortex ring state. Trimming the helicopter in this area would ask for a very accurate measurement of the rate of descent, without any delay, and a huge pilot workload. The helicopter will more probably cross this unstable area and reach higher rate of descents.
3. Around $-1.5 \cdot V_{i0}$, the collective pitch must now decrease again to balance the mass when the rate of descent increases. This is another stable range. It corresponds to the exit of the vortex ring state. The helicopter will stabilize in this area.

This result can be compared with the VRS occurrence as it can be derived from flight tests (Fig.5). When the pilot gradually decreases the collective pitch, the rate of descent starts to build little by little. It corresponds to the first stable range. At some time a very small collective pitch reduction makes the rate of descent increase a lot. The helicopter is then crossing the unstable range and reaches the second stable area.

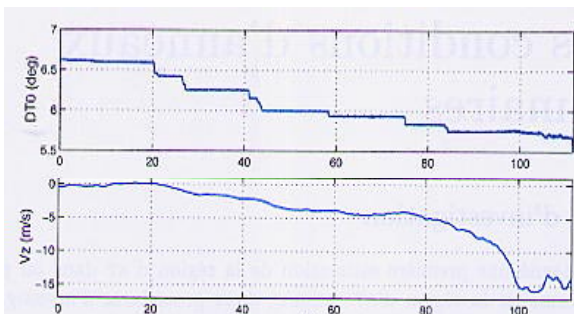


Figure 5 : Evolution of the rate of descent during a flight test for dauphin 6075 across VRS area (taken from Ref 3) versus pitch (DT0).

The vertical velocities for the entrance and the exit of the vortex ring state are in accordance with the experimental ones (Fig.6).

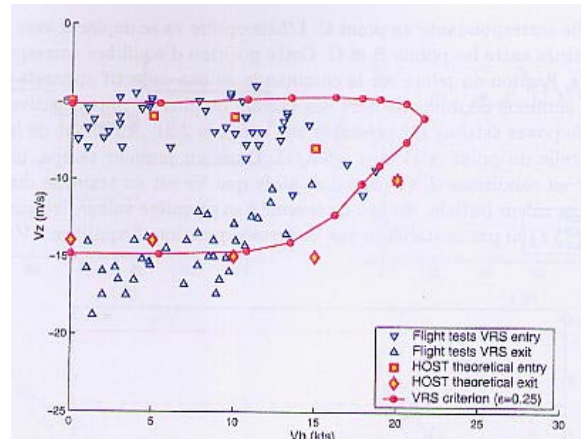


Figure 6 : VRS limits for a Dauphin helicopter - Vertical velocity V_z versus horizontal velocity V_h (taken from Ref 3).

The results provided by this CFD method are thus consistent, from both qualitative and quantitative points of view, with the little experience we have of the vortex ring state phenomenon.

Then, these CFD calculations can be used to try to get a better understanding of the VRS :

1. The rotor thrust appears to be reduced to one third of the level flight value at the same collective pitch when the VRS is fully established (Fig.4). This is directly linked to the vertical acceleration and explains why the entry into VRS is told to be so rapid.
2. Another result of the CFD calculation is the estimation of the collective pitch margin that would be needed to exit the VRS, which is known as the power settling. Starting from the steady high rate of descent stable case, coming back to hover requires reducing the rate of descent and therefore increasing the thrust. An increase by 5° of the collective pitch for AS365 rotor is already necessary to stay with a constant $Z_b=15$ thrust in fully established VRS conditions. Such a large margin is not always available!
3. The flow fields calculated by the elsA CFD code can be used to analyse the VRS phenomenon. Figure 7 shows the vertical velocity on the periodicity plane versus the rate of descent for a fixed collective pitch. It can be

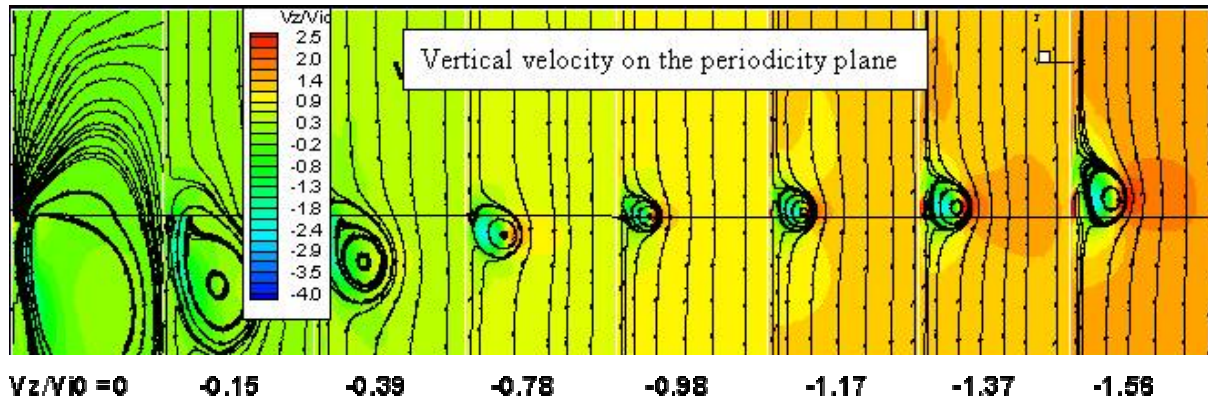


Figure 7 : Normalized vertical velocity on the periodicity plane versus the rate of descent for a 9° collective pitch

noticed that when the rate of descent increases, a recirculation area appears. This recirculation area is the more concentrated and located in the rotor plane with the centre near the blade tip for the minimum thrust and for rate of descent corresponding to $V_z = V_{i0}$. The unstable trim range corresponds to a concentrated vortex located below the rotor and the high rate of descent stable range to a concentrated vortex above the rotor plane. The relative location of this kind of recirculation explains the stable/unstable nature of the equilibrium. The entrance in the VRS zone corresponds to the first interaction of this recirculation area with the blade location.

4. Looking now at the tilt rotor case, at the same normalized thrust ($Z_b = 15$), in order to have the same mean induced velocity of Froude, significant differences with respect to the Dauphin case can be seen onto the exit of the VRS and the power settling aspect (Fig.4). Effectively, if the entrance is not modified, the exit occurs for higher vertical velocity ($2 \cdot V_{i0}$ instead of $1.5 \cdot V_{i0}$) and at least 7° of collective pitch should be required to exit the VRS. The rotor thrust is also reduced to 1/7 in the core of the vortex ring state (Fig 4) instead of 1/3 for AS365 rotor. This seems to indicate that the height loss of the tilt rotor should be more abrupt and more severe. The vortex ring state appears to be more critical for a tilt rotor blade than for a classical helicopter blade. An explanation should be found in the lift distribution : the high twist of the blade leads to a maximum of lift located more inboard where the concentrated recirculation is more influencing.

Isolated rotor in wind tunnel environment

The same flow conditions have been used for the wind tunnel configuration. The boundary conditions are of type 'slipping' on the walls of the wind tunnel. The hover condition requires a preliminary choice on the boundary conditions at the entrance and the exit of the wind tunnel. Two configurations are possible, with a closed or open entrance of the wind tunnel. The first avoids building an induced wind but generates recirculation into the open jet area. The second produces an induced wind, therefore simulating a vertical climbing flight of $0.25 \cdot V_{i0}$ in this configuration. A closed entrance was chosen, because the solution was estimated to be closer to the very low rate of descent case.

In this wind tunnel configuration 10.000 to 12.000 iterations were required to converge correctly, even for hover configuration because recirculation occurs.

In order to evaluate the discrepancies between wind tunnel and free stream conditions, Fig. 8 compares the thrust evolution as a function of the rate of descent for a fixed collective pitch for both configurations. The vortex ring state phenomenon can be identified in the wind tunnel calculation but the entrance and the exit of this phenomenon occur for a lower rate of descent. The minimum thrust is obtained for $0.6 \cdot V_{i0}$ instead of $1 \cdot V_{i0}$ for the free stream configuration but the minimum values of the thrust are close.

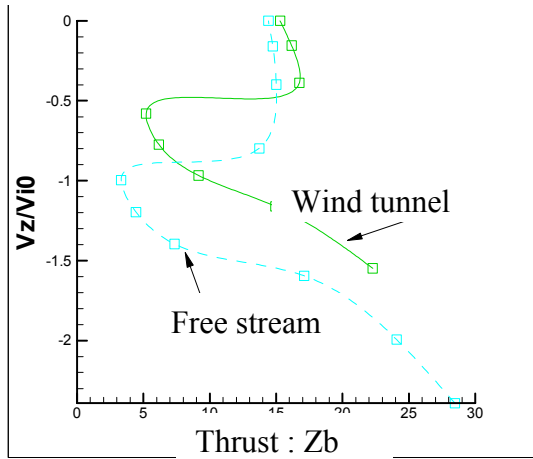


Figure 8 : non-dimensioned thrust versus rate of descent for 9° of collective pitch. Comparison free stream and wind tunnel

The analysis of the local flow velocity (Fig.12) shows that the recirculation phenomenon is the same as for free stream. Due to the proximity of the duct (divergent) below the rotor plane, the recirculation is however pushed towards the rotor plane early. Then the entrance in the VRS occurs earlier. The comparison of the 'paths' of the centres of the recirculation, versus the rate of descent (Fig.12) , shows the same offset than the thrust evolution (Fig.8). There is clearly not enough room between the recirculation area and the wind tunnel jet flow to allow the flow to have the same trajectory than in the free stream configuration. The comparison of the local velocity magnitude at $V_z=V_{i0}$ (minimum of the thrust for free stream) and the streamlines (Fig.9) seems to show that the problem could be linked to the position of the end of the duct (divergent) below the rotor plane. The presence of the duct moves and enlarges the recirculation area. A new calculation without the divergent and convergent (Fig.10) shows effectively an influence on the position of the centre of the recirculation and on the induced velocities, but the recirculation area diameter remains unchanged. The rotor diameter and the rotor plane location in the wind tunnel would need to be varied to find the correct configuration to have no effect of the wind tunnel on the VRS phenomenon.

Thanks to the CFD calculation, we can also highlight a problem of measurement for the upstream velocity magnitude in the Marignane wind tunnel. Indeed, this velocity is usually measured by static pressure sensor in the room around the test section area. Unfortunately, in the VRS configuration there are too much interaction between the open jet and the rotor model to consider the static pressure jet uniform and then equal to the

static pressure in the measurement room (Fig.11).

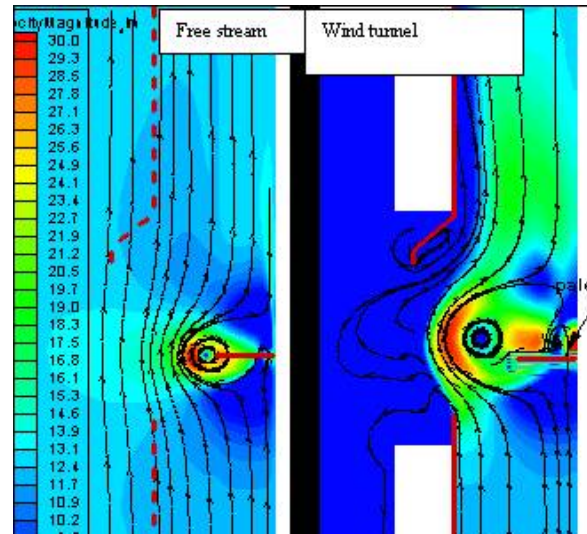


Figure 9 : effect of wind tunnel wall on the velocity magnitude on the periodicity plane for $V_z=V_{i0}$ and pitch=9°.

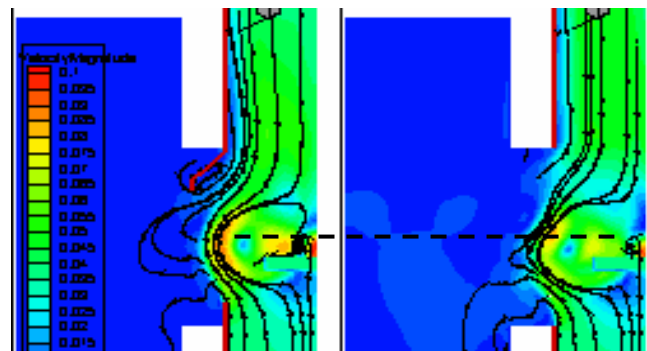


Figure 10 : effect of divergent (red) on the flowfield for $V_z=V_{i0}$ and 9° of collective pitch. Normalized velocity magnitude on periodicity plane.

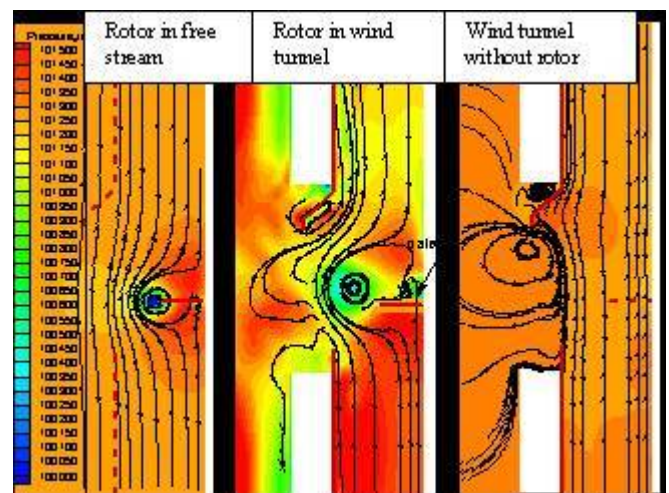


Figure 11 : Static pressure distribution depending on the configuration and calculated by CFD for $V_z=V_{i0}$ and 9° of collective pitch

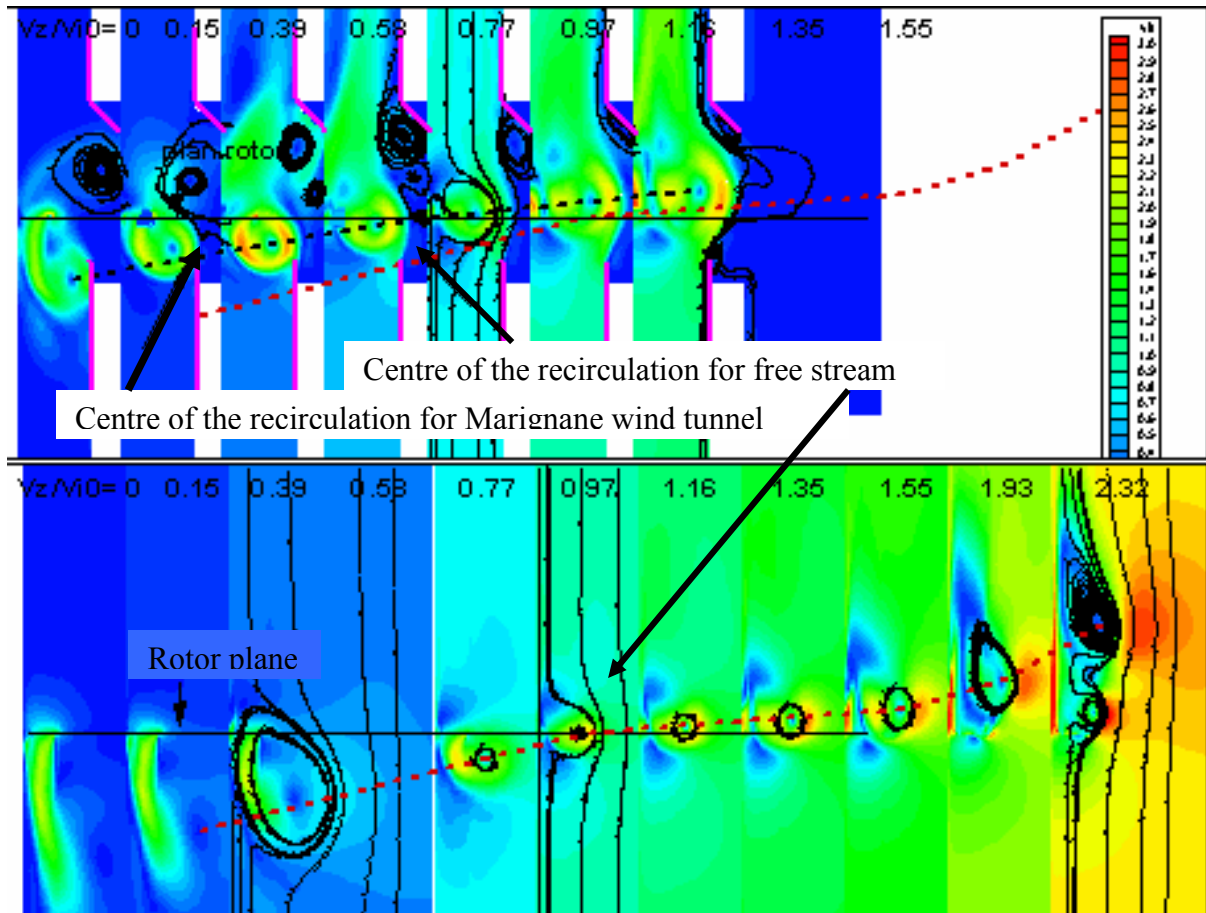


Figure 12 : Comparison of the vortex location for both free stream and wind tunnel configurations versus the rate of descent for a fixed collective pitch (9°). Visualisation of the norm of the velocity normalized by the Froude induced velocity.

Conclusion

The CFD code elsA used for Vortex Ring State computations has provided results that are consistent with the flight experience of this phenomenon.

These computations or the wind tunnel tests they simulated allow trimming a rotor at any point of the VRS range and give access to results that cannot be reached because of the unstable behaviour of the helicopter in such conditions. This allows a better understanding of the VRS..

A CFD comparison between a helicopter and a tilt rotor configuration demonstrated significant discrepancies in terms of VRS behaviour. More work would be needed to identify the influencing factors.

Simulation of a wind tunnel experiment shows that the walls effect cannot be neglected. If it does not fully change the phenomenon, it is

sufficient to significantly affect the quantitative results of the test.

Wind tunnel measurements cannot therefore be directly transferred to real flight conditions. CFD tools can be of great help to reach this goal: once validated against wind tunnel results in a wind tunnel configuration, they can be applied to free stream conditions.

Wind tunnel tests are now necessary to go further in the tool validation. These computations allowed demonstrating that this will not be an easy task. A rotor simulating descent flight has a very strong influence on the wind tunnel flow, which can induce also measurement problems.

The author would like to thank the French DPAC and SPAé for their support.

References

[1] A. D'Alascio, C. Castellin, M. Costes, K. Palhke, '*Aerodynamics of helicopter. Application of the Navier-Stokes codes developed in the framework of the joined German/French program CHANCE*', CEAS 2002

[2] Jeanfaivre G.; Benoit C.; Le Pape M.C. *Improvement of the robustness of the Chimera method*. 32nd AIAA Fluid Dynamics Conference & Exhibit, St. Louis, USA, June 24-26, 2002, AIAA 2002-3290.

[3] J. Jimenez. 'Experimental and numerical study of the behaviour of helicopter in steep descent : vortex ring state phenomenon modelisation'. PhD thesis, ONERA 2002.

[4] P. Beaumier, C. Castellin and G. Arnaud, "Performance Prediction and Flow Field Analysis of Rotors in Hover, Using a Coupled Euler/Boundary Layer method", Proceedings of the 24th European Rotorcraft Forum, Marseille, France, September 1998.